Controlling Fano profiles via conical intersections

Yoav Berlatzky[1,*] and Shachar Klaiman[2,†]
[1]*Department of Physics, Technion–Israel Institute of Technology, Haifa 32000, Israel*
[2]*Shulich Department of Chemistry and Minerva Center for Nonlinear Physics of Complex Systems, Technion–Israel Institute of Technology, Haifa 32000, Israel*

(Received 12 October 2008; revised manuscript received 17 December 2008; published 3 February 2009)

An analytical model for Fano resonances in two-channel systems is presented. By developing a two-potential formula, we find that the line-shape parameter q factors into a background contribution q_b that depends only on the uncoupled channels and an interaction contribution q_i that is affected by the coupling between the channels, revealing how the overall line-shape parameter q may be controlled. In particular, we show how conical intersections of the background phase shifts have an important role in the interplay between q_b and q_i. Finally, control of Fano transmission profiles through q_b and q_i is demonstrated for quantum billiards.

DOI: 10.1103/PhysRevB.79.085303 PACS number(s): 73.23.−b, 33.40.+f, 72.15.Qm, 73.63.Kv

I. INTRODUCTION

Fano resonances are ubiquitous whenever discrete levels interact with a continuum. They have been observed in many areas of physics: atomic and molecular systems,[1,2] quantum dots,[3] carbon nanotubes,[4] microwave billiards,[5] molecular electronic transport,[6] optical ring resonators,[7] and quantum wires.[8] When probed, Fano resonances yield their signature scattering cross-section profile:[1]

$$\sigma \propto \frac{(\epsilon + q)^2}{1 + \epsilon^2}. \tag{1}$$

Here ϵ is the dimensionless reduced energy (which is measured in units of the resonance half width and shifted so that it vanishes at the position of the resonance), while q is the Fano line-shape asymmetry parameter. The latter is proportional to the ratio between the resonant and nonresonant transition amplitudes.[1]

Often the Fano profile is observed in experiments without any theoretical model that explains the sign and magnitude of q. Instead, the value of q is extracted by fitting Eq. (1) to existing data. This has also been the case in many theoretical studies.

Generally, there have been two approaches to calculating the Fano profile. The first gives a heuristic treatment of the Fano model based on Eq. (1) without going into the microscopic details of the interaction between the bound states and the continuum and how it relates to the Fano resonances.[8,9] The second approach uses microscopic models to describe the scattering process. However, these are usually too simplistic and specific[10–12] or overly complex so that they resort to numerical solutions.[13] In either type of microscopic model the Fano mechanism is usually obscured by the details so that a heuristic approach is needed after all.[14,15] The treatment in Ref. 16 is more complete in this respect, showing how in several scenarios the Fano profiles may be explicitly calculated. However, these approaches do not give a complete and general understanding of the Fano q-reversal phenomenon[17,18] nor do they suggest any means of profile control.

Recently, it has been conjectured that the sign of the Fano parameter q might change due to both background resonances and symmetry breaking of the bound-continuum coupling.[19] This has been shown to be plausible.[17] The exact interplay between these two factors remained hidden in previous theoretical studies.[16,18] This turns out to be a crucial point as will be shown below.

The purpose of this work is to provide a detailed microscopic analysis of scattering in a multichannel system with bound states which is on one hand generic, and on the other hand transparent enough so that analytical expressions for the Fano line shapes are within reach. We suggest how to manipulate the asymmetry parameter q by factorizing the S matrix into the *product* of the background and coupling S matrices. This contrasts with previous treatments,[16] where the total scattering matrix was decomposed into a *sum* of background and coupling contributions. Once the S matrix is factored into a product, the resulting line-shape parameter q also factors into

$$q = q_b \cdot q_i. \tag{2}$$

Here q_b is responsible for the contribution of the uncoupled continuum (background), whereas q_i reflects the effect of the interaction between the continuum and the bound state. Our results show the important role played by the background transmission unity peaks, which correspond to conical intersections of the background phase shifts, see Fig. 1. This opens the door to resonance profile control.

This paper is organized as follows. First we show how the S matrix of a general Hamiltonian of the form $H=H^0+V^{\mathrm{I}}+V^{\mathrm{II}}$ may be factorized into the product of two S matrices $S=S^{\mathrm{I}}\cdot S^{\mathrm{II}}$. We call S^{I} the "first-stage" S matrix, which is related to V^{I}, while V^{II} gives rise to the "second-stage" S matrix. This general result is then applied to the present context of Fano model scattering—V^{I} serves as the background scattering potential and V^{II} is the coupling term between the bound state and continuum. We also find how time-reversal invariance (TRI) manifests itself as a constraint on the form of the coupling term V^{II}. Next we derive general analytical expressions for the full two-stage S matrix and describe the interesting geometrical relationship between the background

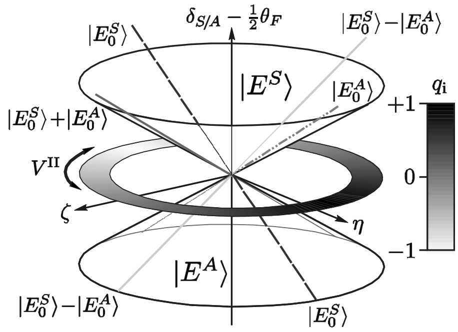

FIG. 1. Parameter space for controlling q near a conical intersection of the background phase shifts. The upper cone corresponds to the state $|E^S\rangle$ and its phase shift δ_S (measured relative to $\frac{1}{2}\theta_F$). To leading order, this state is an azimuth-dependent linear combination of the vertex states $|E_0^{S/A}\rangle$. Changing the coupling V^{II} corresponds to rotating the q_{i} compass wheel.

transmission amplitude and the full two-stage transmission amplitude. Finally, we arrive at our main result and explain how conical intersections of the first-stage (background scattering) phase shifts play an important role in Fano scattering. Control of the Fano q parameter is then demonstrated in a numerical simulation of scattering in an open quantum billiard (QB).

II. FACTORIZATION OF THE SCATTERING MATRIX

In this section we describe the two-stage scattering formalism in general. Assume that the Hamiltonian is of the form $H=H^0+V^{\mathrm{I}}+V^{\mathrm{II}}$. We denote the H^0 states as $|E^\sigma\rangle$, where E is the scattering energy and σ describes additional degeneracies (usually indicating directionality). In the present multichannel context, these states are just plane waves,

$$\langle x|E^\sigma\rangle = \frac{e^{\sigma ikx}}{\sqrt{2\pi k}}, \tag{3}$$

where $\sigma=\pm$ and k is the wave number corresponding to the scattering energy $E=\frac{1}{2}k^2>0$. Here we are working with a Schrödinger equation with units chosen so that $\hbar=m=1$ and assume unbiased leads. Given an arbitrary unit of length, the corresponding unit of energy is (length^{-2}). Note, however, that the rest of the derivation in this section is general and does not depend on the explicit form of these states.

The first scattering stage is due to V^{I} with Møller wave operators $\Omega_\pm^{\mathrm{I}}$ resulting in the outgoing

$$|E_{(+)}^\sigma\rangle \equiv \Omega_+^{\mathrm{I}}|E^\sigma\rangle \tag{4a}$$

and incoming

$$|E_{(-)}^\sigma\rangle \equiv \Omega_-^{\mathrm{I}}|E^\sigma\rangle \tag{4b}$$

first-stage scattering states. The first-stage scattering operator $S^{\mathrm{I}}\equiv\Omega_-^{\mathrm{I}\dagger}\Omega_+^{\mathrm{I}}$ has matrix elements in the basis of H^0's states given by

$$\langle E^\sigma|S^{\mathrm{I}}|E'^{\sigma'}\rangle = \langle E_{(-)}^\sigma|E'^{\sigma'}_{(+)}\rangle = S^{\mathrm{I}}_{\sigma\sigma'}(E)\,\delta(E-E'). \tag{5}$$

Now assume that the addition of the coupling V^{II} is described by the second-stage wave operators $\Omega_\pm^{\mathrm{II}}$ acting on the first-stage states. This scattering process is schematically described in Fig. 2. It is clear that H's total S matrix with respect to H^0's states is

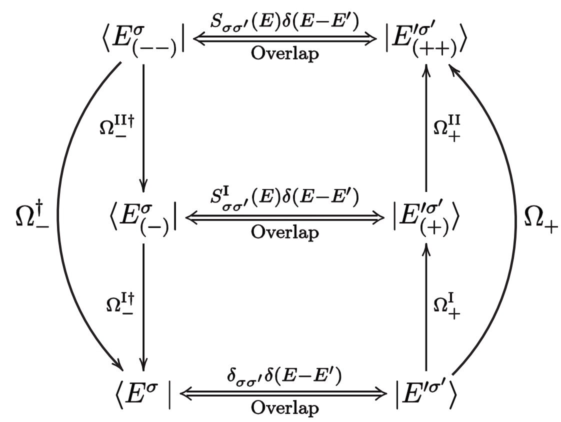

FIG. 2. Two-stage scattering schema in terms of wave operators. Note the overlap relations.

$$S=\Omega_-^{\mathrm{I}\dagger}\Omega_-^{\mathrm{II}\dagger}\Omega_+^{\mathrm{II}}\Omega_+^{\mathrm{I}}. \tag{6}$$

However, in the present context this approach is inconvenient for the following reason. Note that the first-stage wave operators $\Omega_\pm^{\mathrm{I}}$ act on the same states $|E^\sigma\rangle$, whereas the second-stage wave operator Ω_+^{II} acts on $|E_{(+)}^\sigma\rangle$, but Ω_-^{II} acts on $|E_{(-)}^\sigma\rangle$. In this sense the operator $\Omega_-^{\mathrm{II}\dagger}\Omega_+^{\mathrm{II}}$ does not have the usual interpretation as a scattering operator, while the first-stage scattering operator S^{I} does not explicitly appear in Eq. (6).

When using the Lippmann-Schwinger equation (LSE) or the Fano model to describe the second-stage interaction, it is easier to describe the second-stage scattering process in terms of only one set of first-stage states, usually taken to be the outgoing states $|E_{(+)}^\sigma\rangle$. Therefore assume that the action of V^{II} is embodied in the scattering operator $\widetilde{S}^{\mathrm{II}}$ with matrix elements

$$\langle E_{(+)}^\sigma|\widetilde{S}^{\mathrm{II}}|E'^{\sigma'}_{(+)}\rangle = \widetilde{S}^{\mathrm{II}}_{\sigma\sigma'}(E)\,\delta(E-E'). \tag{7}$$

Note that we are using the *tilde* ($\sim$) to emphasize that this scattering operator's relation to the previous wave operators is as of yet not established. The same holds for the second-stage states and wave operators in Fig. 3 which describe the total scattering process.

Now let us see how this relates to the total S matrix described in Fig. 2. The two-stage S-matrix elements are given by

$$S_{\sigma\sigma'}\delta(E-E') = \langle E^\sigma|S|E'^{\sigma'}\rangle = \langle E_{(-)}^\sigma|\Omega_-^{\mathrm{II}\dagger}\Omega_+^{\mathrm{II}}|E'^{\sigma'}_{(+)}\rangle. \tag{8}$$

Next, expressing the first-stage continuum projector using either set of first-stage states in conjunction with the overlap relation in Eq. (5) allows one to write

$$\begin{tikzcd}
& \langle \tilde{E}^{\sigma}_{(+-)}| \arrow[rr, Leftrightarrow, "\tilde{S}^{\mathrm{II}}_{\sigma\sigma'}(E)\delta(E-E')", "\text{Overlap}"'] \arrow[dr, "\tilde{\Omega}^{\mathrm{II}\dagger}_{-}"'] & & |\tilde{E}'^{\sigma'}_{(++)}\rangle \\
\langle E^{\sigma}_{(-)}| \arrow[rr, Leftrightarrow, "S^{\mathrm{I}}_{\sigma\sigma'}(E)\delta(E-E')", "\text{Overlap}"'] \arrow[d, "\Omega^{\mathrm{I}\dagger}_{-}"'] & & |E'^{\sigma'}_{(+)}\rangle \arrow[ur, "\tilde{\Omega}^{\mathrm{II}}_{+}"'] & \\
\langle E^{\sigma}| \arrow[rr, Leftrightarrow, "\delta_{\sigma\sigma'}\delta(E-E')", "\text{Overlap}"'] & & |E'^{\sigma'}\rangle \arrow[u, "\Omega^{\mathrm{I}}_{+}"'] &
\end{tikzcd}$$

FIG. 3. Two-stage scattering schema in terms of S matrices.

$$\mathbb{1}^{\mathrm{I}}_{(+)} = \mathbb{1}^{\mathrm{I}}_{(-)} = \int dE \sum_{\sigma,\sigma'} |E^{\sigma}_{(-)}\rangle S^{\mathrm{I}}_{\sigma\sigma'} \langle E^{\sigma'}_{(+)}|.$$

Note that this is a passive change in basis transformation in the first-stage continuum subspace that just seems to have the same matrix elements as the operator S^{I}, but of course it is not the first-stage scattering operator, $S^{\mathrm{I}} \neq \mathbb{1}^{\mathrm{I}}_{(\pm)}$. Inserting the above projection operator to the right-hand side (RHS) of Eq. (8) yields

$$S_{\sigma\sigma'}\delta(E-E') = \sum_{\sigma''} S^{\mathrm{I}}_{\sigma\sigma''} \langle E^{\sigma''}_{(+)}|\Omega^{\mathrm{II}\dagger}_{-}\Omega^{\mathrm{II}}_{+}|E'^{\sigma'}_{(+)}\rangle,$$

which is just the definition of $\tilde{S}^{\mathrm{II}}$. Therefore we find that

$$S_{\sigma\sigma'} = \sum_{\sigma''} S^{\mathrm{I}}_{\sigma\sigma''} S^{\mathrm{II}}_{\sigma''\sigma'}, \tag{9}$$

where we have now removed the tildes ($\sim$) since these turn out to be the same second-stage wave operators. To clarify this last point, note that the matrix elements of S^{II} are defined as

$$S^{\mathrm{II}}_{\sigma\sigma'}(E)\delta(E-E') = \langle E^{\sigma}_{(+)}|\Omega^{\mathrm{II}\dagger}_{-}\Omega^{\mathrm{II}}_{+}|E'^{\sigma'}_{(+)}\rangle,$$

while the total S matrix has elements

$$S_{\sigma\sigma'}(E)\delta(E-E') = \langle E^{\sigma}_{(-)}|\Omega^{\mathrm{II}\dagger}_{-}\Omega^{\mathrm{II}}_{+}|E'^{\sigma'}_{(+)}\rangle.$$

Finally, observe that if we had defined S^{II} relative to the incoming first-stage states $|E^{\sigma}_{(-)}\rangle$, then the order of matrix multiplication in Eq. (9) would be reversed.

III. GENERAL TWO-CHANNEL MODEL

Although, in general there might be an infinite number of channels involved in the scattering process, the essential physics resulting in a Fano profile is often captured by a two-channel description of the scattering process—this was also the underlying assumption in the original analysis of Fano.[1] We assume a single-particle TRI multichannel system where only the lowest channel is open and the scattering energy is in the vicinity of an isolated bound state in the second channel with other bound states energetically separate so that we may disregard them.

The next step is to combine the results of Sec. II and obtain the full two-stage scattering matrix. The two-channel Hamiltonian is partitioned as $H=H^0+V^{\mathrm{I}}+V^{\mathrm{II}}$, which treats scattering as a conceptual two-stage process. The first scattering stage, with S matrix S^{I}, describes scattering due to V^{I} relative to the H^0 states in the first uncoupled channel. The potential V^{I} also accounts for the bound state $|\varphi\rangle$ at energy E_{φ} in the second channel. The second scattering stage S^{II} describes the scattering of the H^0+V^{I} states under the influence of interchannel interaction V^{II}, which turns the bound state into a resonance. The second stage is accounted for by the Fano model. The latter is used to give an approximate description of the coupling of the first-stage scattering states to the bound state in the closed second channel, all the while taking the TRI constraint into account.

To be more specific, the quasi-one-dimensional multichannel formalism is based on expanding the wave function as $\Psi=\Sigma_n \psi_n(x)|n^x\rangle$, where $\{|n^x\rangle\}$ is the local x-dependent transverse basis (assumed nondegenerate) and $\psi_n(x)$ are the channel wave functions. When the channel wave functions are written in vectorial notation, the Schrödinger equation assumes the form[20]

$$\left\{-\frac{1}{2}[\partial_x + A(x)]^2 + V^t(x)\right\}\psi(x) = E\psi(x). \tag{10}$$

The covariant gauge connection is the anti-Hermitian matrix $A_{mn}(x) \equiv \langle m^x|\partial_x n^x\rangle$, while $V^t_{mn}(x) \equiv \langle m^x|H(x)+\frac{1}{2}\partial_x^2|n^x\rangle$ are the transverse Hamiltonian matrix elements. Since the underlying parameter space is just the real line, the fiber bundle is trivial, and we may set the gauge condition $A_{nn}=0$.

There are two common approaches to choosing the local transverse basis. The simplest is to use a constant transverse basis, usually taken to be that of the leads.[21] This gives a vanishing gauge connection, but in most cases the resulting V^t is pretty complicated. The Born-Oppenheimer (BO) expansion is a more refined approach, where the $\{|n^x\rangle\}$ are transverse eigenstates giving a diagonal V^t with eigenvalues that define the adiabatic potential surfaces. This formulation naturally lends itself to the partitioning $H=H^0+V^{\mathrm{I}}+V^{\mathrm{II}}$, where $V^{\mathrm{I}}=V^t$ embodies the BO adiabatic surface potentials and V^{II} are the nonadiabatic coupling terms.[22] The latter are given by what is called the "derivative coupling," obtained by expanding the covariant kinetic term to $-\frac{1}{2}\langle m^x|\partial_x^2 n^x\rangle - \langle m^x|\partial_x n^x\rangle\partial_x$. Of course, any other partitioning scheme may also be acceptable as long as V^{I} pertains to the uncoupled channels and V^{II} to the interchannel coupling.

We begin the analysis of the two coupled channels by analyzing the scattering matrix of the open one-dimensional (1D) channel, i.e., the first-stage scattering matrix S^{I}. In the presence of TRI, S^{I} is of the form

$$S^{\mathrm{I}} = \begin{pmatrix} t & r^- \\ r^+ & t \end{pmatrix} = \begin{pmatrix} t & re^{-i\delta_r} \\ re^{+i\delta_r} & t \end{pmatrix}. \tag{11}$$

Here we have used the slightly unconventional notation where no scattering corresponds to the unit matrix.[23] The ambiguity in the above decomposition may be removed by the constraint $-\pi/2 < \delta_r \leq \pi/2$.[24] Note that this matrix may be parametrized by

$$t = e^{i\theta_F} \cos \Delta\theta, \tag{12a}$$

$$r = ie^{i\theta_F} \sin \Delta\theta, \tag{12b}$$

where the angles θ_F and $\Delta\theta$ will be fully defined shortly. The S matrix in Eq. (11) may be diagonalized by

$$S^{\mathrm{I}} = U \begin{pmatrix} e^{2i\delta_S} & 0 \\ 0 & e^{2i\delta_A} \end{pmatrix} U^{\dagger}, \tag{13}$$

where we have made a specific choice of phases in the eigenvector matrix

$$U = \frac{1}{\sqrt{2}} \begin{pmatrix} e^{-i\delta_S-(i/2)\delta_r} & -ie^{-i\delta_A-(i/2)\delta_r} \\ e^{-i\delta_S+(i/2)\delta_r} & ie^{-i\delta_A+(i/2)\delta_r} \end{pmatrix}. \tag{14}$$

We also define the eigenstates of S^{I},

$$|E^S\rangle = \frac{e^{-i\delta_S}}{\sqrt{2}} [e^{-(i/2)\delta_r}|E^+\rangle + e^{+(i/2)\delta_r}|E^-\rangle] \tag{15a}$$

$$|E^A\rangle = \frac{e^{-i\delta_A}}{i\sqrt{2}} [e^{-(i/2)\delta_r}|E^+\rangle - e^{+(i/2)\delta_r}|E^-\rangle], \tag{15b}$$

which are H^0 eigenstates, and their first-stage relatives

$$|E^S_{(+)}\rangle = \Omega^{\mathrm{I}}_+|E^S\rangle = \frac{e^{-i\delta_S}}{\sqrt{2}} [e^{-(i/2)\delta_r}|E^+_{(+)}\rangle + e^{+(i/2)\delta_r}|E^-_{(+)}\rangle], \tag{16a}$$

$$|E^A_{(+)}\rangle = \Omega^{\mathrm{I}}_+|E^A\rangle = \frac{e^{-i\delta_A}}{i\sqrt{2}} [e^{-(i/2)\delta_r}|E^+_{(+)}\rangle - e^{+(i/2)\delta_r}|E^-_{(+)}\rangle]. \tag{16b}$$

The eigenvalues also satisfy

$$e^{2i\delta_S} = t + r \tag{17a}$$

$$e^{2i\delta_A} = t - r, \tag{17b}$$

hence the notations $\delta_{S/A}$ refer to the symmetric/antisymmetric combinations of t and r. Finally,

$$\theta_F = \delta_S + \delta_A, \tag{18a}$$

$$\Delta\theta = \delta_S - \delta_A, \tag{18b}$$

where θ_F is the Friedel angle.[25] Also, the first-stage transmission and reflection coefficients are

$$\mathbf{T}^{\mathrm{I}} = \cos^2(\delta_S - \delta_A), \tag{19a}$$

$$\mathbf{R}^{\mathrm{I}} = \sin^2(\delta_S - \delta_A). \tag{19b}$$

For brevity, the discussion of the above parametrization, the asymptotic behavior of the states $|E^{S/A}_{(+)}\rangle$, and the proper gauge conventions is postponed to Appendix A.

We now turn to treat the coupling between the first-stage and the second-stage scatterings. Assume that the first-stage outgoing scattering states are coupled by V^{II} to the bound state in the second channel with matrix elements

$$\langle\varphi|V^{\mathrm{II}}|E^{\sigma}_{(+)}\rangle = v^{\sigma}_E. \tag{20}$$

It is more convenient to use the bound-state couplings to the states $|E^{S/A}_{(+)}\rangle$ given in Eqs. (16a) and (16b). Using TRI, see Appendix B, one can show that the different couplings are connected in the following way:

$$\begin{pmatrix} v^S_E \\ v^A_E \end{pmatrix} = U^t \begin{pmatrix} v^+_E \\ v^-_E \end{pmatrix},$$

where we have defined the couplings to $|E^{S/A}_{(+)}\rangle$ as

$$v^S_E = \langle\varphi|V^{\mathrm{II}}|E^S_{(+)}\rangle,$$

$$v^A_E = \langle\varphi|V^{\mathrm{II}}|E^A_{(+)}\rangle,$$

and the matrix U is given in Eq. (14).

According to the Fano model, the second-stage S matrix S^{II} has elements

$$[S^{\mathrm{II}}]_{\mathbf{F}} = \begin{pmatrix} e^{2i\delta_E} & 0 \\ 0 & 1 \end{pmatrix}, \tag{21}$$

where the subscript "**F**" indicates that the elements are taken relative to the "Fano" basis $\mathbf{F} = \{|E^{\parallel}_{(+)}\rangle, |E^{\perp}_{(+)}\rangle\}$. These orthonormal basis states are the linear combinations of the first-stage scattering states $|E^{\pm}_{(+)}\rangle$ such that $|E^{\perp}_{(+)}\rangle$ does not couple via V^{II} to the second channel bound state $|\varphi\rangle$. In other words, the states $\{|E^{\parallel}_{(+)}\rangle, |E^{\perp}_{(+)}\rangle\}$ are chosen so that

$$v_E = \langle\varphi|V^{\mathrm{II}}|E^{\parallel}_{(+)}\rangle, \tag{22a}$$

$$0 = \langle\varphi|V^{\mathrm{II}}|E^{\perp}_{(+)}\rangle, \tag{22b}$$

with $v_E \equiv \sqrt{|v^+_E|^2 + |v^-_E|^2}$. The Fano phase shift is given as

$$\tan(\delta_E) = -\frac{\frac{1}{2}\Gamma(E)}{E - E_{\varphi} - \Delta(E)}. \tag{23}$$

Here we have used the usual definitions

$$\Gamma(E) = 2\pi|v_E|^2, \tag{24a}$$

$$\Delta(E) = \frac{1}{2\pi}\mathcal{P}\int dE' \frac{\Gamma(E')}{E - E'}. \tag{24b}$$

If v_E varies slowly enough as a function of E then it is reasonable to approximate $\Gamma(E)$ and $\Delta(E)$ using their values at the bound-state energy E_{φ},[26] i.e., we assume a constant scattering background.

Thus, in order to get the total S-matrix elements $S = S^{\mathrm{I}} \cdot S^{\mathrm{II}}$, all that is left is to express the change in basis transformation from the first-stage scattering state basis $|E^{\pm}_{(+)}\rangle$ to the Fano basis. Since the interchannel couplings $v^{\pm}_E$ need to adhere to the TRI constraint Eq. (B3), it is easiest if we work according to the $v^{S/A}_E$ parametrization, which only requires the latter to be real. Therefore, in terms of the states $|E^{S/A}_{(+)}\rangle$,

$$|E^{\parallel}_{(+)}\rangle = \frac{1}{v_E}(v^S_E|E^S_{(+)}\rangle + v^A_E|E^A_{(+)}\rangle),$$

$$|E^{\perp}_{(+)}\rangle = \frac{1}{v_E}(-v^A_E|E^S_{(+)}\rangle + v^S_E|E^A_{(+)}\rangle).$$

By defining the rotation matrix

$$R(\alpha) \equiv \frac{1}{v_E}\begin{pmatrix} v^S_E & -v^A_E \\ v^A_E & v^S_E \end{pmatrix} \equiv \begin{pmatrix} \cos\alpha & -\sin\alpha \\ \sin\alpha & \cos\alpha \end{pmatrix}, \tag{25}$$

we find that in the first-stage scattering state basis $\mathbf{S} = \{|E^+_{(+)}\rangle, |E^-_{(+)}\rangle\}$ the second-stage S matrix has elements

$$[S^{\mathrm{II}}]_{\mathbf{S}} = UR[S^{\mathrm{II}}]_{\mathbf{F}}R^\dagger U^\dagger.$$

Finally, the total two-stage S matrix, which we implicitly express in the H^0 scattering basis, is

$$S = S^{\mathrm{I}}S^{\mathrm{II}} = e^{i(\delta_S+\delta_A+\delta_E)}\begin{pmatrix} \tau & ie^{-i\delta_r}\rho^- \\ ie^{+i\delta_r}\rho^+ & \tau \end{pmatrix}, \tag{26}$$

with

$$\tau = \cos^2\alpha\cos(\delta_S - \delta_A + \delta_E) + \sin^2\alpha\cos(\delta_S - \delta_A - \delta_E), \tag{27a}$$

$$\rho^{\pm} = \cos^2\alpha\sin(\delta_S - \delta_A + \delta_E) + \sin^2\alpha\sin(\delta_S - \delta_A - \delta_E) \pm 2i\sin\alpha\cos\alpha\sin\delta_E. \tag{27b}$$

By defining

$$\delta'_\rho = \arg(\rho^+),$$

we see that the two-stage S-matrix parameters are related to the first-stage matrix by

$$\theta_F \mapsto \Theta_F = \theta_F + \delta_E,$$

$$\delta_r \mapsto \delta_\rho = \delta_r + \delta'_\rho,$$

$$\Delta\theta \mapsto \Delta\Theta = \arccos\left(\frac{1}{\tau}\right).$$

These last results have important implications. First note that magnitude of the transmission amplitude τ looks like the linear interpolation with ratio $\cos^2\alpha:\sin^2\alpha$ between the magnitude of transmission amplitudes corresponding to a δ_E change in either δ_S or δ_A. This linear interpolation picture also applies to the real part $\mathrm{Re}\{\rho^{\pm}\}$, but it does not carry over to the magnitude of the reflection amplitude due to the nonlinear relation $\tau^2+|\rho^{\pm}|^2=1$. The "extra slack" is taken up by the imaginary part $\mathrm{Im}\{\rho^{\pm}\}$. As we shall see next, the "linear interpolation" of the transmission amplitudes is what always ensures the transmission zeros in the Fano line shapes, while the extra slack term is what inhibits the reflection zeros.

The full two-stage S-matrix elements have an interesting geometric representation. We defer, however, the discussion of these properties to Appendix C.

Next, let us look at the Fano line shapes. The ratio of the full two-stage transmission amplitude to that of the first stage assumes the almost familiar form

$$\frac{\mathbf{T}}{\mathbf{T}^{\mathrm{I}}} = \frac{(\epsilon + q_b \cdot q_i)^2}{1+\epsilon^2}, \tag{28a}$$

with the usual dimensionless Fano parameters

$$\epsilon = -\cot\delta_E = \frac{E - E_\varphi - \Delta_E}{\frac{1}{2}\Gamma_E},$$

$$q_b = \tan(\delta_S - \delta_A) = \pm\sqrt{\frac{\mathbf{R}^{\mathrm{I}}}{\mathbf{T}^{\mathrm{I}}}},$$

and the additional factor

$$q_i = \cos(2\alpha).$$

The subscript on q_b emphasizes that this is only the background contribution—this distinction is important when discussing the q-reversal phenomenon since the overall line-shape asymmetry factor is a product of the background contribution q_b and the coupling contribution q_i.

We assume that the coupling v_E is weak with δ_E changing rapidly enough so that the first-stage scattering process may be considered as a static background. In this case one takes the parameter q_b as an energy-independent constant where the phase shifts δ_S and δ_A are evaluated at a scattering energy matching that of the bound state E_φ. Similarly we find that the ratio of reflection amplitudes is

$$\frac{\mathbf{R}}{\mathbf{R}^{\mathrm{I}}} = \frac{[\epsilon - q_b^{-1}\cos(2\alpha)]^2 + (1+q_b^{-2})\sin^2(2\alpha)}{1+\epsilon^2}. \tag{28b}$$

In terms of the above dimensionless parameters, the actual two-stage transmission and reflection coefficients are

$$\mathbf{T} = \frac{[\epsilon + q_b\cos(2\alpha)]^2}{(1+\epsilon^2)(1+q_b^2)}, \tag{29a}$$

$$\mathbf{R} = \frac{[\epsilon - q_b^{-1}\cos(2\alpha)]^2}{(1+\epsilon^2)(1+q_b^{-2})} + \frac{\sin^2(2\alpha)}{1+\epsilon^2}. \tag{29b}$$

From here it is clear that there will always be transmission zeros, regardless of the asymmetry parameter q_b or the coupling ratio angle α, yet reflection zeros are obtained only if the bound state $|\varphi\rangle$ couples exclusively to either $|E^S_{(+)}\rangle$ or $|E^A_{(+)}\rangle$. The general form of the Fano line shape is described in Fig. 4.

The transmission (reflection) coefficient assumes the symmetric Breit-Wigner Lorentzian form if the first-stage transmission (reflection) coefficient is zero. Note, however, that when $\mathbf{T}^{\mathrm{I}}=0$ the transmission Lorentzian has a maximal value of $\cos^2(2\alpha)$, while the reflection Lorentzian reaches unity in the $\mathbf{R}^{\mathrm{I}}=0$ case. Finally, the reflection coefficient also assumes the Lorentzian form if the bound state $|\varphi\rangle$ is coupled with equal strength to the $|E^{S/A}_{(+)}\rangle$ states but the Lorentzian range only covers the interval from $\mathbf{R}^{\mathrm{I}}$ to one, i.e., full transmission is not possible unless $q_b=0$ in such a case. These results are summarized in Fig. 5. All of these special cases may be directly inferred from Fig. 11.

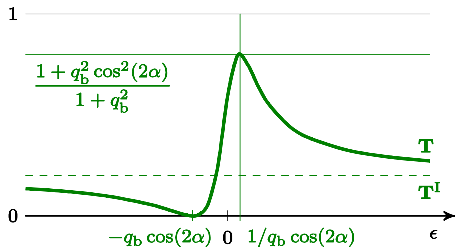

FIG. 4. (Color online) The general form of the transmission Fano line shape. The transmission zero is obtained at $\epsilon_0 = q_b\cos(2\alpha)$, while the maximal transmission value $\frac{1+q_b^2\cos^2(2\alpha)}{1+q_b^2}$ is attained at $\epsilon_{\max}=\frac{1}{q_b\cos(2\alpha)}$. The transmission approaches the asymptotic value $\mathbf{T}^{\mathrm{I}}$ as $|\epsilon|\to\infty$.

IV. CONICAL INTERSECTION

The line-shape asymmetry parameter q factors into a background contribution q_b that solely depends on V^{I} and a coupling interaction contribution q_i, which may be controlled using V^{II}. However, neither q_b nor q_i is gauge invariant when taken alone—only their product is. This subtlety will be treated in detail in what follows. Understanding how V^{II} controls q_i is a simple affair—the decoupled first-stage surfaces V^{I} are not affected, so that q_b and the states $|E^{S/A}\rangle$ remain constant regardless of the specific gauge used to define them [here we have dropped the (+) subscript to keep the notation uncluttered]. On the other hand, modifying V^{I} may affect both q_b and q_i, an effect that is predominant in the vicinity of background unity transmission peaks, as we now show.

Suppose that at a scattering energy $E=E_0$ the background transmission reaches a unity peak, implying that $\delta_S^0=\delta_A^0$. Here we accent values at the transmission peak by a 0 so that $S_0^{\mathrm{I}} = e^{i\theta_F^0}\mathbb{1}$. Assume throughout that δ_S approaches δ_A with a leading order linear in $E-E_0$. Since the background S matrix is degenerate at this energy, there are no preferred eigenvectors. However, we may choose to use the states in Eqs. (16a) and (16b) that evolve smoothly from those obtained for values $E<E_0$, which we denote as $|E_0^{S/A}\rangle$. These limiting states are associated with an angle δ_r^0, which is just the limit of δ_r as E_0 is approached from below. Note that by a suitable choice of gauge (i.e., choosing which point to label $x=0$), it is possible to set $\delta_r^0=0$.

Now we modify V^{I} near the background transmission unity at E_0, leading to three types of infinitesimal deformations of the background S matrix,

$$dS^{\mathrm{I}} = iS_0^{\mathrm{I}}[\mathbb{1}d\xi + \Sigma_r^0(\sigma_x d\eta + \sigma_y d\zeta)],$$

where $\Sigma_r^0=\exp(-i\sigma_z\delta_r^0)$. Note the absence of a σ_z *generator* which breaks TRI. The ξ deformation affects only θ_F, keeping the degeneracy intact, and it does not change the eigenvectors nor does it change the position of the transmission peak that still reaches unity. The η deformation acts through the σ_x generator and affects $\Delta\theta$. This removes the degeneracy, but to leading order $|E_0^{S/A}\rangle$ are still its eigenstates since this is how we defined them for $E<E_0$. It also shifts the position of the unity peak in the transmission spectrum away from E_0. Finally, the ζ deformations change the height of the peak while keeping its position. More importantly, ζ deformations are orthogonal to the η deformations in the sense that the degeneracy is removed so that to leading order the eigenvectors are proportional to $|E_0^S\rangle \pm |E_0^A\rangle$.

The effect of these deformations on the first-stage S matrix may be described as a conical intersection of the phase shifts $\delta_{S/A}$ in the $\eta\zeta$ plane, schematically depicted in Fig. 1. Here the actual eigenstates $|E^{S/A}\rangle$ are defined according to the $\Delta\theta \geq 0$ gauge, i.e., $|E^S\rangle$ is on the upper cone. The leading-order behavior of this state depends on the position in the parameter space. On one side of the η axis $|E^S\rangle \sim |E_0^S\rangle$, while on the other it crosses over to $|E^S\rangle \sim |E_0^A\rangle$. Similarly, along the ζ axis it crosses over from $|E_0^S\rangle + |E_0^A\rangle$ to $|E_0^S\rangle - |E_0^A\rangle$.[27]

The interplay between q_b and q_i can now be understood in terms of such conical intersections. The $\Delta\theta \geq 0$ gauge choice ensures that $q_b > 0$ on the conical surface (equaling zero at the vertex), so that up to appropriate parametrization-dependent scale factors, q_b corresponds to the radial distance from the vertex in parameter space. In many cases it is also reasonable to assume that the bound-state coupling to the $|E_0^{S/A}\rangle$ states remains (relatively) constant near the intersection. However, due to the behavior of $|E^{S/A}\rangle$ that changes according to the position in parameter space, the actual couplings to the bound state also change so that q_i depends on the azimuthal angle cosine. The initial coupling to the $|E_0^{S/A}\rangle$ states may be modified through V^{II}, and in effect this rotates the "compass wheel" in Fig. 1, i.e., $q_i \equiv 1$ points in a different direction in the $\eta\zeta$ plane.

V. QUANTUM BILLIARD EXAMPLE

The above analysis of the Fano profile can be applied to any system where the scattering can be accurately described by an effective two coupled-channel model. Recently, Fano resonances have been studied extensively in connection with QBs, see e.g., Refs. 5 and 28. We therefore choose to exemplify the above factorization of the Fano q parameter on such

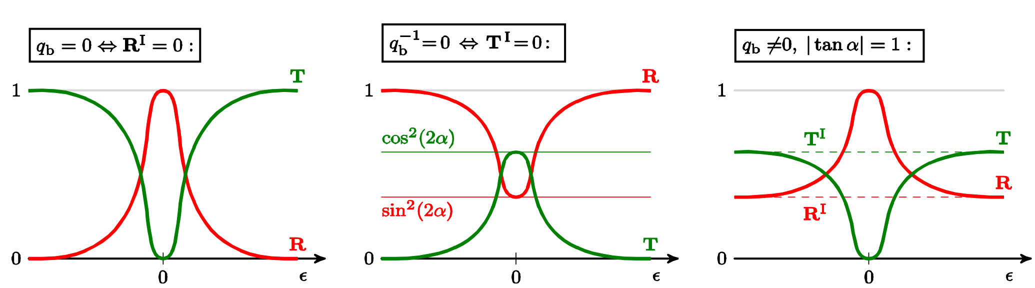

FIG. 5. (Color online) The special cases where Lorentzian line shapes are obtained.

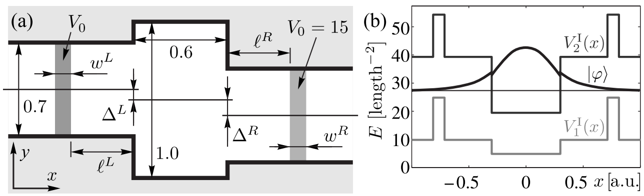

FIG. 6. (a) Geometry of the quantum billiard with leads used to demonstrate control of Fano q reversal. Length is measured in arbitrary units, while the energy scale is in units of (length^{-2}) (b) The first two adiabatic surfaces $V^{\mathrm{I}}_{1,2}(x)$ and the second surface bound state $|\varphi\rangle$.

a QB. The application to other physical systems is straightforward.

Usually, the QB is composed of an access lead from which the electrons impinge upon the main billiard, typically the part associated with a quantum dot, and an exit lead. The electron-scattering problem in QBs can be cast into a one-dimensional coupled-channel problem,[17] where the channels are taken to be the energies of the modes in the transverse direction, and the interchannel interactions are due to the nonadiabatic couplings.[29]

Control of q will be demonstrated on the QB depicted in Fig. 6(a). It consists of a rectangular cavity connected to leads that have two-potential barriers of constant heights V_0, with widths $w^{L/R}$ and distances from the cavity $\ell^{L/R}$. The leads are offset from the cavity centerline by $\Delta^{L/R}$. In this specific example, the barriers are used to modify the first-stage S matrix S^{II}, while the nonadiabatic couplings that define S^{II} are controlled by the lead offsets. The first two adiabatic potential surfaces (channels) are depicted in Fig. 6(b).

The significance of a conical intersection is demonstrated near the unity transmission peak at E_0=27.35 for a parity symmetric V^{I} obtained by setting $w^{L/R}$=0.1 and $\ell^{L/R}$=0.295. This is convenient since the symmetry ensures that the states $|E_0^{S/A}\rangle$ have respective even and odd parities in the $\delta_r\equiv 0$ gauge. The background V^{I} is modified to control the line-shape parameter q near the conical intersection. Taking

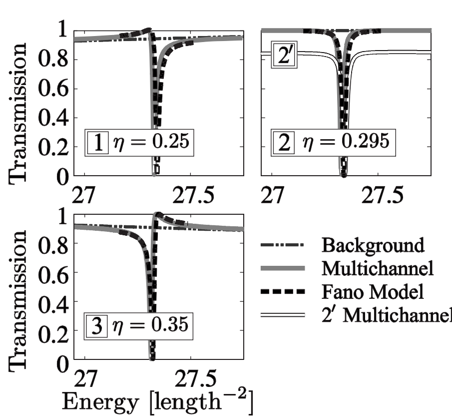

FIG. 7. Multichannel, background, and analytical line shapes obtained for various V^{I} configurations of the potential barrier parameters (see Table I). Note the excellent fit between the numerically exact transmission profiles and those calculated according to our analytical model.

TABLE I. QB potential barrier parameters for various configurations in the $\eta\zeta$ parameter space. Note that they only affect the background channel.

Configuration no.	w^L	ℓ^L	ℓ^R	w^R
1	0.1	0.250	0.250	0.1
2	0.1	0.295	0.295	0.1
3	0.1	0.350	0.350	0.1
2′	0.1	0.295	0.255	0.3

$\Delta^{L/R}$=0.01 ensures that V^{II} couples $|\varphi\rangle$ exclusively to $|E_0^S\rangle$ by symmetry. We choose $\eta=\ell^L=\ell^R$, which preserves parity and ζ deformations that break this symmetry. Removing the parity symmetry from the QB can be achieved by changing the ratios ℓ^L/ℓ^R and w^L/w^R.

Figure 7 depicts the Fano profiles resulting from the numerically exact multichannel calculation,[30] our analytical model, and the background contributions for several sets of QB parameters, see Table I. In all cases note the excellent fit between the actual multichannel calculations and the line shapes predicted by our model. This series of calculations corresponds to two q-reversal paths in parameter space depicted in Fig. 8. The first path along the η axis goes from points 1, with $q<0$, to 3 ($q>0$) by passing exactly through the background unity transmission peak at point 2, where q_b=0. Note that for point 1 the transmission peak energy has moved to the right of the resonance, while the opposite happens at point 3. The second path goes from points 1 to 3 through 2′ which breaks parity symmetry. This point has a subunity background transmission peak, corresponding to a pure ζ deformation. As expected from the conical intersection, at this point in parameter space the states $|E^{S/A}\rangle$ are similar to $|E_0^S\rangle\pm|E_A^S\rangle$. This implies equal coupling to the bound state, so that q_i=0, giving a symmetric dip with the novelty of a less than unity background.

The above control of the Fano q parameter was accomplished by varying the value of the background factor, q_b. This was achieved through the modification of the transmission unities of the background channel by changing the positions and widths of the potential barriers in the leads. Note, however, that similar control could have been achieved had we placed potential wells in the leads instead of potential

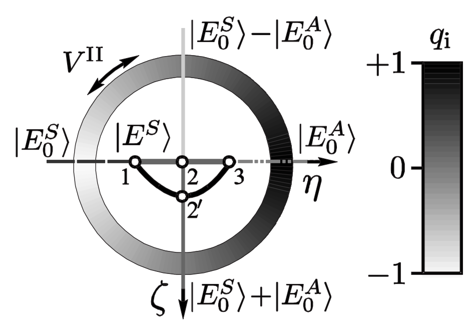

FIG. 8. The configurations in Table I correspond to two paths in parameter space where q-reversal occurs: $1\rightarrow 2\rightarrow 3$ and $1\rightarrow 2'\rightarrow 3$. The overall line-shape parameter q vanishes at the intermediate points; q_b=0 at point 2 while q_i=0 at 2′.

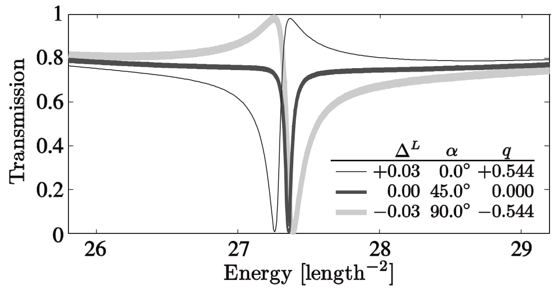

FIG. 9. Variation in the nonadiabatic couplings V^{II} gives q reversal due to the change in the coupling angle α, and hence q_i. The inset table summarizes analytical values calculated from the model.

barriers. In fact, one could use any variation in the background channel that controls the positions of the transmission unities to modify the Fano q parameter.

Control of q may also be affected through V^{II}, which directly controls q_i, while $q_b>0$ remains constant. In the language of conical intersections the V^{I} parameters remain constant, so that q reversal is achieved through a rotation of the compass wheel. This type of control works irrespective of the position in parameter space relative to conical intersections. For simplicity, again we choose a parity symmetric V^{I}, this time with $\ell^{L/R}=0.4125$ and $w^{L/R}=0.1$ so that $q_b=0.544$ throughout. Now we vary $\Delta^L=-0.03\mapsto 0.03$ while holding $\Delta^R=0.03$. The results of the numerically exact multichannel calculations are depicted in Fig. 9.

VI. CONCLUSIONS

The Fano resonance profile greatly facilitates the analysis of a scattering cross section. The simple line-shape formula allows the characterization of a resonance in the cross section via a single parameter, i.e., the Fano q parameter. The greatest strength of the Fano profile is in its applicability to a myriad of physical systems. Although it is well known that the parameter q serves as a measure of the ratio between the resonant and nonresonant pathways, its exact connection with the microscopic details of the scattering process remained rather obscure. By developing a two-potential formula the precise contribution of the different microscopic pathways to the Fano parameter q was made clear.

We have presented an analytical model for Fano resonances in coupled two-channel systems, where we found that the Fano line-shape parameter q factors into background and interaction contributions. The model gives accurate predictions for the actual transmission line shapes in the local approximation. Even when this assumption must be dropped, as is the case in many experiments, our model still allows for a qualitative understanding of the resulting line-shape parameter.[17] Moreover, it also provides insight to the relation between conical intersections of the background phase shifts, the coupling interaction, and the overall line-shape parameter q. The full control of q, although specifically demonstrated for a quantum billiard example, is applicable to other systems where a Fano profile is observed.

ACKNOWLEDGMENTS

The authors acknowledge useful discussions with N. H. Lindner and N. Moiseyev. This work was funded in part by the fund for promotion of research at the Technion. S.K. acknowledges the support of the Israel ministry of science, culture and sports.

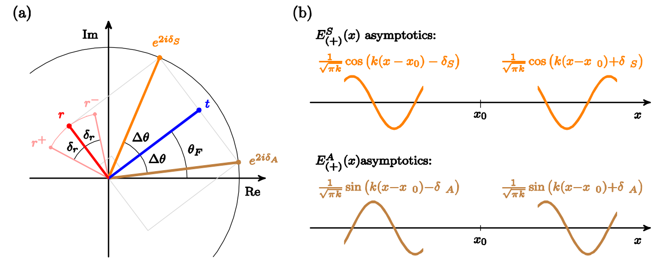

FIG. 10. (Color online) (a) Parametrization of the 1D TRI S matrix on the unit circle. (b) First-stage scattering state phase shifts and asymptotics.

APPENDIX A: ADDITIONAL PROPERTIES OF THE FIRST-STAGE SCATTERING MATRIX

The parametrization of the 1D S matrix, see Eqs. (12a) and (12b), is a generalization of the analysis for a parity-symmetric 1D TRI potential.[31,32] There $\delta_r\equiv 0$ and $e^{2i\delta_{S/A}}$ had parity-symmetric/antisymmetric eigenvector wave functions, while here δ_r is a function of the scattering energy. Additionally, one may easily verify that in the present case the eigenvectors have symmetric/antisymmetric boundary conditions relative to the point

$$x_0(E)=\frac{\delta_r}{2k},$$

where k is the lead wave number associated with the scattering energy $E=\frac{1}{2}k^2$. The choice of phases in the definitions of the scattering states in Eqs. (16a) and (16b) ensures that the wave functions $E^{S/A}_{(+)}(x)$ are real. Finally, relative to the point x_0 one obtains the phase shifts $\delta_{S/A}$ induced by the scattering operator S^{I} on either eigenvector. All of the above relations between the S-matrix parameters are summarized in Fig. 10(a). Figure 10(b) shows the $E^{S/A}_{(+)}$ scattering state boundary conditions and phase shifts.

From this parametrization it is clear that the transmission amplitude is a gauge-invariant property, as well as the combinations $\delta_S+\delta_A$ and $|\delta_S-\delta_A|$. On the other hand, the phase controlled by δ_r depends on the choice of origin for the x axis as well as picking one of the possible parametrization choices $\pm r$. The latter is equivalent to deciding which of the S-matrix eigenvalues is $e^{2i\delta_S}$. The gauge-fixing constraint $-\pi/2<\delta_r\leq\pi/2$ picks one of the possible choices $\pm r$ such that symmetry point in a parity-symmetric potential is $x_0\equiv 0$ and the parity-symmetric states correspond to δ_S. Another convenient gauge choice is $\Delta\theta\geq 0$, which is useful for describing the conical intersection of the eigenvalues.

APPENDIX B: TIME-REVERSAL INVARIANCE CONSTRAINTS

This appendix shows how TRI finds its expression as a constraint on the coupling of the first-stage scattering states to the bound state in the second channel. The S matrix for a multichannel TRI problem satisfies

$$\Sigma_x S \Sigma_x = S^t, \tag{B1}$$

with "t" denoting transpose and Σ_x being the block form of the Pauli matrix σ_x.[21,33] Assume that the first-stage outgoing scattering states are coupled by V^{II} to the bound state in the second channel with matrix elements

$$\langle \varphi | V^{\mathrm{II}} | E^{\sigma}_{(+)} \rangle = v^{\sigma}_E. \tag{B2}$$

Next note that since V^{I} is a TRI potential, the first-stage scattering wave functions are related by complex conjugation

$$E^{+}_{(+)}(x) = [E^{-}_{(-)}(x)]^*,$$

$$E^{-}_{(+)}(x) = [E^{+}_{(-)}(x)]^*.$$

Since we assume that V^{II} is also TRI, while the 1D bound state $|\varphi\rangle$ may be chosen to be represented by a real wave function, we find that

$$(v^{+}_E)^* = \langle \varphi | V^{\mathrm{II}} | E^{-}_{(-)} \rangle,$$

$$(v^{-}_E)^* = \langle \varphi | V^{\mathrm{II}} | E^{+}_{(-)} \rangle.$$

Finally, using the overlap relations in Eq. (5) to express the incoming states, using the outgoing states yields the TRI constraint on the coupling elements

$$\begin{pmatrix} v^{-}_E \\ v^{+}_E \end{pmatrix} = S^{\mathrm{I}} \begin{pmatrix} (v^{+}_E)^* \\ (v^{-}_E)^* \end{pmatrix}. \tag{B3}$$

Using the unitarity of S^{I} gives that up to an indeterminate phase $e^{i\eta}$,

$$e^{i\eta} \begin{pmatrix} -(v^{+}_E)^* \\ (v^{-}_E)^* \end{pmatrix} = S^{\mathrm{I}} \begin{pmatrix} -v^{-}_E \\ v^{+}_E \end{pmatrix}.$$

By combining the above two equations and taking the determinant

$$\det \begin{pmatrix} v^{-}_E & -e^{i\eta}(v^{+}_E)^* \\ v^{+}_E & e^{i\eta}(v^{-}_E)^* \end{pmatrix} = \det \left[S^{\mathrm{I}} \begin{pmatrix} (v^{+}_E)^* & -v^{-}_E \\ (v^{-}_E)^* & v^{+}_E \end{pmatrix} \right],$$

we find that the phase is just $\det(S^{\mathrm{I}})$ so that we get an alternate form for the TRI constraint

$$\det(S^{\mathrm{I}}) \begin{pmatrix} -(v^{+}_E)^* \\ (v^{-}_E)^* \end{pmatrix} = S^{\mathrm{I}} \begin{pmatrix} -v^{-}_E \\ v^{+}_E \end{pmatrix}. \tag{B4}$$

Next we will find a suitable parametrization of v^{+}_E and v^{-}_E so that the constraint equation is satisfied. There are several ways of doing this. First, since Eq. (B3) is reminiscent of an eigenvalue equation, it is easy to guess that the couplings may be parametrized as

$$\begin{pmatrix} v^{+}_E \\ v^{-}_E \end{pmatrix} = \frac{e^{+i\delta_S}}{\sqrt{2}} \begin{pmatrix} e^{+(i/2)\delta_r} \\ e^{-(i/2)\delta_r} \end{pmatrix} v^{S}_E + \frac{ie^{+i\delta_A}}{\sqrt{2}} \begin{pmatrix} -e^{+(i/2)\delta_r} \\ e^{-(i/2)\delta_r} \end{pmatrix} v^{A}_E, \tag{B5}$$

where v^{S}_E and v^{A}_E are real. Let us verify this formally. Define the matrices

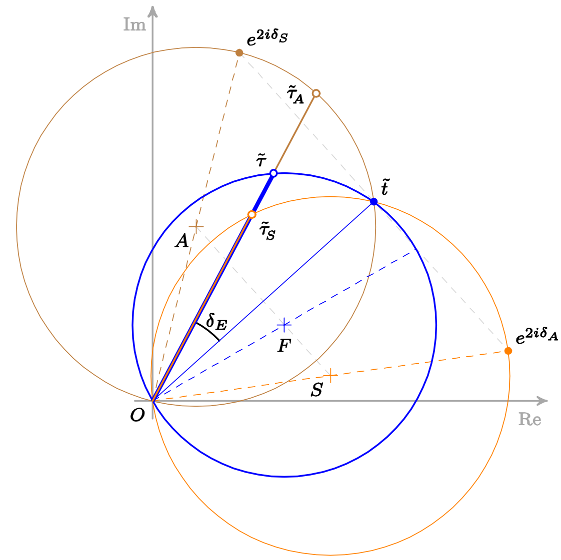

FIG. 11. (Color online) Geometry of the full two-stage scattering transmission amplitude. The transmission amplitude $\tilde{\tau}$ is the linear interpolation with ratio $\cos^2\alpha:\sin^2\alpha$ between the amplitudes $\tilde{\tau}_S$ and $\tilde{\tau}_A$. For $\delta_E=0$ these coincide with the background transmission $\tilde{t}=t\exp\{i(\delta_S+\delta_A)\}$. Assuming a constant background as δ_E increases to π, $\tilde{\tau}_S$ and $\tilde{\tau}_A$ move on circles with unit diameter centered at S and A. High-school geometry shows that $\tilde{\tau}$ moves on a circle centered at F. This point is on the line connecting S to A such that the segment lengths $|SF|$ and $|FA|$ also have the ratio $\cos^2\alpha:\sin^2\alpha$.

$$\sqrt{S^{\mathrm{I}}} = U \begin{pmatrix} e^{i\delta_S} & 0 \\ 0 & e^{i\delta_A} \end{pmatrix} U^{\dagger},$$

$$\sqrt{\Sigma_x} = \frac{1}{2} \begin{pmatrix} 1+i & 1-i \\ 1-i & 1+i \end{pmatrix},$$

so that we may rewrite Eq. (B3) as

$$\Sigma_x (\sqrt{S^{\mathrm{I}}})^{\dagger} \Sigma_x \begin{pmatrix} v^{+}_E \\ v^{-}_E \end{pmatrix} = \Sigma_x \sqrt{S^{\mathrm{I}}} \begin{pmatrix} (v^{+}_E)^* \\ (v^{-}_E)^* \end{pmatrix}.$$

Next, using the fact that $\sqrt{S^{\mathrm{I}}}$ is TRI so that it satisfies the relation in Eq. (B1) and also $(\sqrt{\Sigma_x})^{\dagger} = (\sqrt{\Sigma_x})^*$ gives

$$(\sqrt{\Sigma_x})^* (\sqrt{S^{\mathrm{I}}})^* \begin{pmatrix} v^{+}_E \\ v^{-}_E \end{pmatrix} = \sqrt{\Sigma_x}\sqrt{S^{\mathrm{I}}} \begin{pmatrix} (v^{+}_E)^* \\ (v^{-}_E)^* \end{pmatrix},$$

i.e., the above combination is real. This means that for real parameters $v^{S/A}_E$ we may write

$$\begin{pmatrix} v^{+}_E \\ v^{-}_E \end{pmatrix} = (\sqrt{\Sigma_x})^t (\sqrt{S^{\mathrm{I}}})^t A \begin{pmatrix} v^{S}_E \\ v^{A}_E \end{pmatrix},$$

where for convenience we have inserted the real matrix

$$A = \frac{1}{\sqrt{2}} \begin{pmatrix} \cos\frac{1}{2}\delta_r + \sin\frac{1}{2}\delta_r & -\cos\frac{1}{2}\delta_r + \sin\frac{1}{2}\delta_r \\ \cos\frac{1}{2}\delta_r - \sin\frac{1}{2}\delta_r & \cos\frac{1}{2}\delta_r + \sin\frac{1}{2}\delta_r \end{pmatrix}.$$

This replicates the parametrization given in Eq. (B5).

Finally, another way of approaching the TRI coupling constraint is to look at the bound-state couplings to the states $|E^{S/A}_{(+)}\rangle$. For the moment let us call these couplings

$$v^S_E = \langle\varphi|V^{\mathrm{II}}|E^S_{(+)}\rangle,$$

$$v^A_E = \langle\varphi|V^{\mathrm{II}}|E^A_{(+)}\rangle,$$

and as we shall next show, these definitions coincide with the previous ones. According to Eqs. (16) and (B2),

$$\begin{pmatrix} v^S_E \\ v^A_E \end{pmatrix} = U^t \begin{pmatrix} v^+_E \\ v^-_E \end{pmatrix},$$

or in other words

$$\begin{pmatrix} v^+_E \\ v^-_E \end{pmatrix} = U^* \begin{pmatrix} v^S_E \\ v^A_E \end{pmatrix},$$

bringing us back to the parametrization in Eq. (B5).

APPENDIX C: GEOMETRIC PROPERTIES OF THE FULL TWO-STAGE S MATRIX

The full two-stage S-matrix elements have an interesting geometric representation. For example, Fig. 11 shows the complex plane path that the transmission amplitude $\tilde{\tau} = \tau \exp\{i(\delta_S + \delta_A + \delta_E)\}$ traces out as the Fano phase shift δ_E increases from 0 to π when the scattering energy passes the shifted bound-state energy $E_\varphi + \Delta$. Assuming a constant scattering background, simple geometry shows that $\tilde{\tau}$ traces a circle that passes through the origin, hence the transmission is zero. However, unless α is a multiple of $\pi/2$ (implying that $|\varphi\rangle$ couples exclusively to either $|E^S_{(+)}\rangle$ or $|E^A_{(+)}\rangle$), this circle diameter is less than unity, so that reflection zeros are not attained. If the background is not constant, then the circles get distorted, but as long as the resonance is fairly isolated, the path still passes through the origin, demonstrating that transmission zeros are generic.

*yoavbe@tx.technion.ac.il
†shachark@tx.technion.ac.il
[1] U. Fano, Phys. Rev. **124**, 1866 (1961).
[2] S. T. Cornett, H. R. Sadeghpour, and M. J. Cavagnero, Phys. Rev. Lett. **82**, 2488 (1999).
[3] J. Göres, D. Goldhaber-Gordon, S. Heemeyer, M. A. Kastner, H. Shtrikman, D. Mahalu, and U. Meirav, Phys. Rev. B **62**, 2188 (2000).
[4] J. Kim, J.-R. Kim, Jeong-O Lee, J. W. Park, H. M. So, N. Kim, K. Kang, K.-H. Yoo, and J.-J. Kim, Phys. Rev. Lett. **90**, 166403 (2003).
[5] S. Rotter, U. Kuhl, F. Libisch, J. Burgdörfer, and H.-J. Stöckmann, Physica E **29**, 325 (2005).
[6] A. Chakrabarti, Phys. Lett. A **366**, 507 (2007).
[7] L. Y. Mario and M. K. Chin, Opt. Quantum Electron. **38**, 1143 (2007).
[8] W. Porod, Z. Shao, and C. S. Lent, Phys. Rev. B **48**, 8495 (1993).
[9] P. J. Price, Appl. Phys. Lett. **62**, 289 (1993).
[10] P. S. Deo, S. Bandopadhyay, and S. Das, Int. J. Mod. Phys. B **16**, 2247 (2002).
[11] B. F. Bayman and C. J. Mehoke, Am. J. Phys. **51**, 875 (1983).
[12] C. S. Kim, A. M. Satanin, Y. S. Joe, and R. M. Cosby, Phys. Rev. B **60**, 10962 (1999).
[13] Y. Takagaki and D. K. Ferry, Phys. Rev. B **44**, 8399 (1991).
[14] Ch. Kunze, Phys. Rev. B **48**, 14338 (1993).
[15] Z. Shao, W. Porod, and C. S. Lent, Phys. Rev. B **49**, 7453 (1994).
[16] J. U. Nöckel and A. D. Stone, Phys. Rev. B **50**, 17415 (1994).
[17] S. Klaiman, N. Moiseyev, and H. R. Sadeghpour, Phys. Rev. B **75**, 113305 (2007).
[18] T. Nakanishi, K. Terakura, and T. Ando, Phys. Rev. B **69**, 115307 (2004).
[19] A. C. Johnson, C. M. Marcus, M. P. Hanson, and A. C. Gossard, Phys. Rev. Lett. **93**, 106803 (2004).
[20] S. Ulreich and W. Zwerger, Europhys. Lett. **41**, 117 (1998).
[21] Pier A. Mello and Narendra Kumar, *Quantum Transport in Mesoscopic Systems: Complexity and Statistical Fluctuations* (Oxford University Press, Oxford, 2004).
[22] F. A. Maaø, I. V. Zozulenko, and E. H. Hauge, Phys. Rev. B **50**, 17320 (1994).
[23] The present notation is related to the standard one by the transformation $\Sigma_x S \Sigma_x$.
[24] There is another gauge choice giving a unique decomposition which will be discussed further on.
[25] J. Friedel, Philos. Mag. **43**, 153 (1952).
[26] C. Cohen-Tannoudji, J. Dupont-Roc, and G. Grynberg, *Atom-Photon Interactions: Basic Processes and Applications* (Wiley, New York, 1992).
[27] One might naturally ask what topological phase is associated with these conical intersections. The answer is that δ_r shifts by 2π for each cycle that encircles a vertex, and this serves as the basis for adiabatic quantum swimming/pumping; see for example, J. E. Avron, B. Gutkin, and D. H. Oaknin, Phys. Rev. Lett. **96**, 130602 (2006).
[28] J. F. Song, Y. Ochiai, and J. P. Bird, Appl. Phys. Lett. **82**, 4561 (2003); M. Mendoza and P. A. Schulz, Phys. Rev. B **71**, 245303 (2005).
[29] L. S. Cederbaum, in *Conical Intersections*, edited by W. Domcke, D. R. Yarkony, and H. Köppel (World Scientific, Singapore, 2004).
[30] W.-D. Sheng, J. Phys.: Condens. Matter **9**, 8369 (1997).
[31] A. H. Kahn, Am. J. Phys. **29**, 77 (1961).
[32] P. J. Price, Phys. Rev. B **38**, 1994 (1988).
[33] A. V. Tartakovski, Phys. Rev. B **52**, 2704 (1995).